IGA of a Photocathode

1 Geometry

The current geometry was derived from the technical drawings in [1]. Some simplifications were made especially regarding the inner part of the electrode, such that the geometry may be modeled as being rotationally symmetric. The dimensions of the electrode, puck, puck elevator, vacuum chamber and insulator were derived from Figure A.1, A.2, A.3, A.4 and A.6 in [1] respectively. The geometry of the vacuum chamber was also simplified to reduce the computational domain and the reduced insulator geometry is in part based on the drawing in Figure 5.7 of the thesis. The boundary conditions were retrieved from Table 5.1 in [1] and the relative permittivity of the insulator was taken from an existing CST model to be 9.4.

The geometry is depicted in fig. 1. The numbers refer to the individual patches in the context of IGA. The patch boundaries are indicated by the black lines. The red lines represent homogeneous Dirichlet boundary conditions, the blue lines inhomogeneous Dirichlet boundary conditions with a value of -60kV and the green lines indicate homogeneous Neumann boundaries. According to the technical drawings patch 10 as well as parts of patches 7 and 8 should consist of insulator material. In the case of patch 10 this is already included in the model and it could also be added in the other cases.

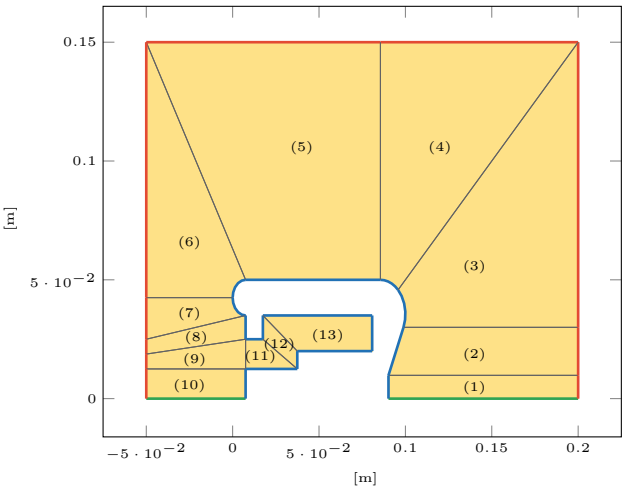

Figure 1: Photocathode geometry and boundary conditions.

2 Electrostatic Potential and Electric Field

The solution for the electrostatic potential is shown in fig. 2. Fig. 3 depicts the absolute value of the electric field. Both of the solutions were computed with $p = 5$ as the degree of the basis functions and $n_{\text{sub}} = 16$ as the number of elements that each knot vector is uniformly split into. The boundary between patches 5 and 6 seems to be visible in the solution of the electric field. The sharp corners on the left boundary of patch 11 seem to also lead to a similiar issue. To give an idea of the error associated with this behavior the absolute error per element will be shown in the following section.

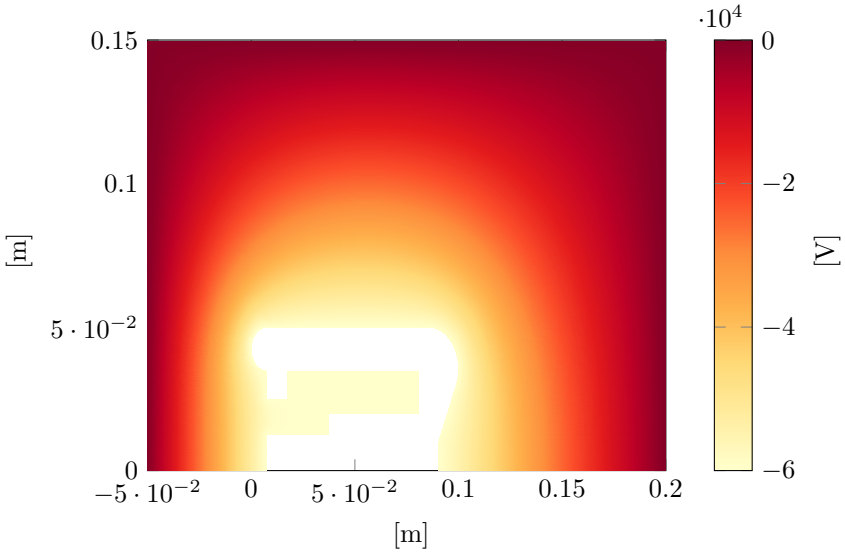

Figure 2: Electrostatic potential.

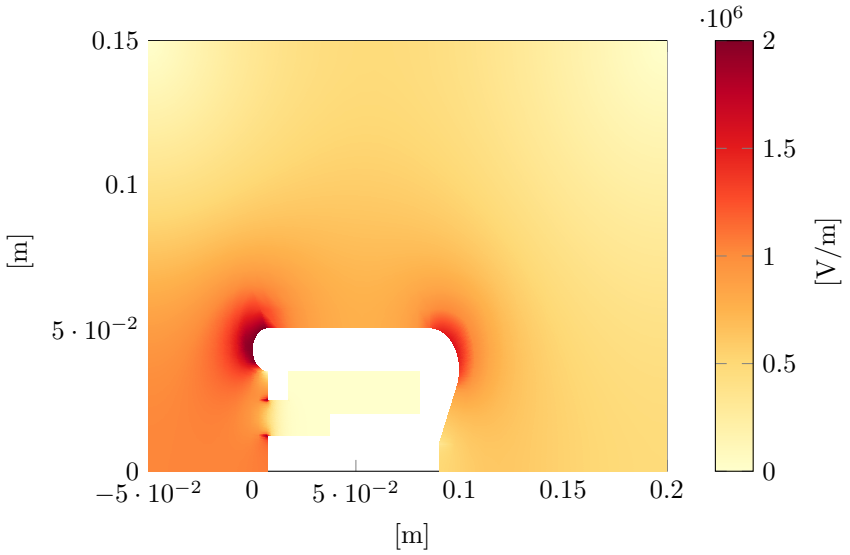

Figure 3: Absolute value of the electric field.

3 Convergence Study

The convergence studies investigate the accuracy of the solution while increasing the number of elements per patch. (Akin to h-refinement in classical FEA) Since no analytic solution exists we used a reference with $n_{\text{sub}} = 256$ and $p = 4$ as a comparison. The errors are computed as

$$e_{L^2} = \frac{\|\varphi_{\text{it}} - \varphi_{\text{ref}}\|_{L^2}}{\|\varphi_{\text{ref}}\|_{L^2}} \tag{1}$$

and (2)

$$e_{H^1} = \frac{\|\varphi_{\text{it}} - \varphi_{\text{ref}}\|_{H^1}}{\|\varphi_{\text{ref}}\|_{H^1}} \tag{3}$$

where

$$\|\varphi\|_{H^1} = \sqrt{\|\varphi\|_{L^2}^2 + \|\nabla\varphi\|_{L^2}^2}. \tag{4}$$

Here φ denotes the electrostatic potential. The integrals associated with the L^2-norm are evaluated using a quadrature rule defined on each element of a given patch.

The degrees of the basis functions are given in the legend, as well as theoretical limits for the convergence rates. They are given by $p + 1$ in the case of the L^2-norm (electrostatic potential) and p in the case of the H^1-norm (electric field). As seen in fig. 4 and fig. 5 we observe convergence, however the convergence rate appears to be limited.

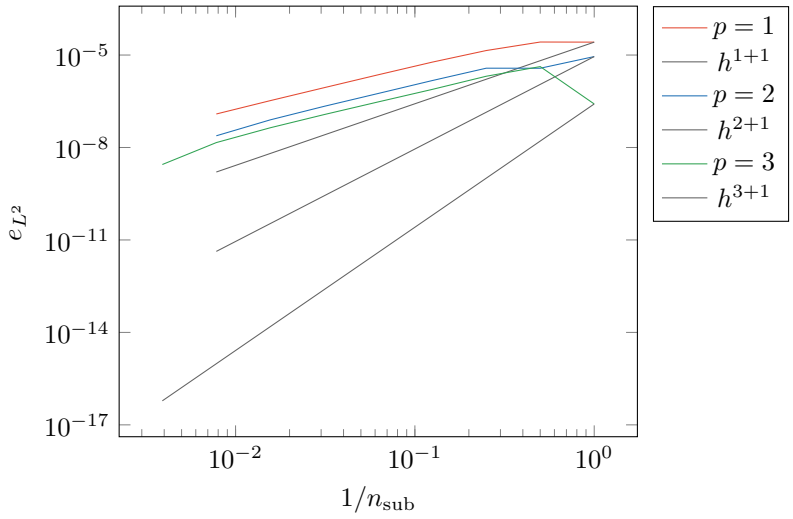

Figure 4: Convergence of L^2-norm.

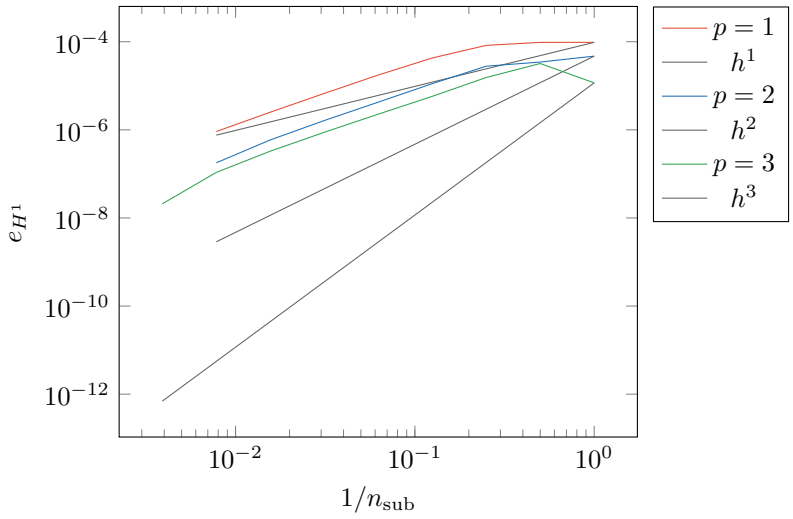

Figure 5: Convergence of H^1-norm.

Lastly the issue described in sec. 2 was investigated by displaying the absolute error of the eletric field on every individual element of the mesh. In the case of fig. 6 we chose $n_{\text{sub}} = 256$ and $p = 3$ were used for the iterative solution and compared with a reference using $n_{\text{sub}} = 256$ and $p = 4$. The figure shows absolute error on each element on a logarithmic scale.

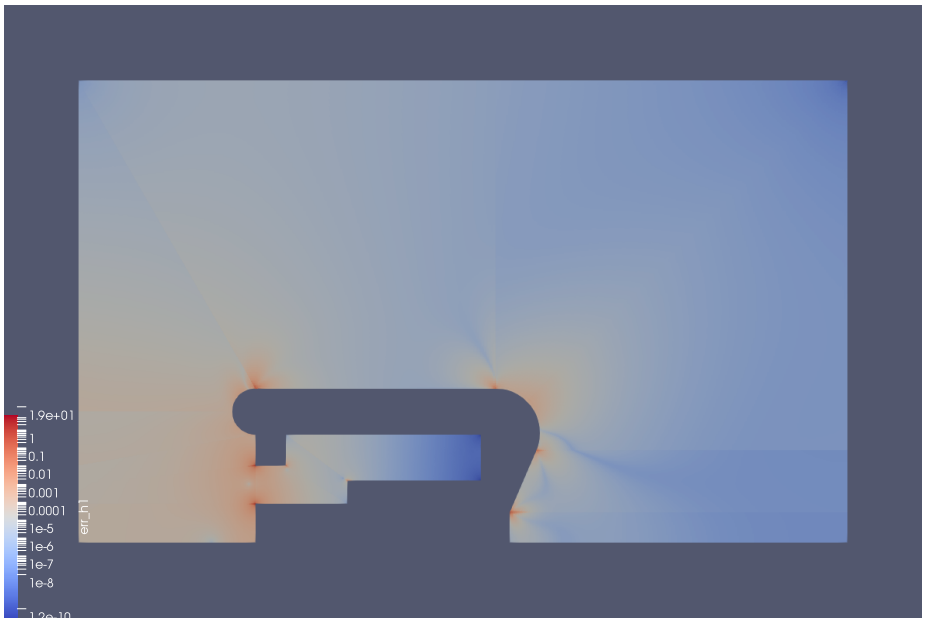

Figure 6: Absolute error of the electric field on every element.

References

[1] Martin Espig. *Development, construction and characterization of a variable repetitive spin-polarized electron gun with an inverted-geometry insulator.* PhD thesis, Technische Universität Darmstadt, 2016.